



OPEN

Cannabinoid receptor 2 deletion influences social memory and synaptic architecture in the hippocampus

Joanna Agnieszka Komorowska-Müller, Kishore Aravind Ravichandran, Andreas Zimmer[✉] & Britta Schürmann

Although the cannabinoid receptor 2 (CB₂R) is often thought to play a role mainly outside the brain several publications unequivocally showed the presence of CB₂R on hippocampal principal neurons. Activation of CB₂R produced a long-lasting membrane potential hyperpolarization, altered the input/output function of CA2/3 principal neurons and produced alterations in gamma oscillations. However, other cellular, molecular and behavioral consequences of hippocampal CB₂R signaling have not been studied in detail. Here we demonstrate that the deletion of CB₂ leads to a highly significant increase in hippocampal synapsin-I expression levels and particle density, as well as increased vesicular GABA transporter (vGAT) levels. This phenotype was restricted to females and not observed in males. Furthermore, we demonstrate an impairment of social memory in CB₂ deficient mice. Our results thus demonstrate that the lack of CB₂R leads to changes in the hippocampal synaptic landscape and reveals an important sex-specific difference in endocannabinoid signaling. This study supports a significant role of the CB₂R in modulation of different types of memory despite its low expression levels in the brain and provides more insight into a sex-specific role of CB₂R in synaptic architecture.

The endocannabinoid system (ECS) consists of endocannabinoids, their receptors, and their synthesizing and degrading enzymes. The two main cannabinoid receptors are: cannabinoid receptor 1 (CB₁R) and cannabinoid receptor 2 (CB₂R, encoded by the gene *Cnr2*). CB₁R has been extensively studied in the brain, whereas CB₂R for a long time has been regarded as the peripheral cannabinoid receptor, present mostly on endocrine and immune cells^{1,2}. Its characterization in the brain has been a challenge due to its low baseline expression and a lack of reliable antibodies³. Initially, CB₂R was detected in the brain during pathological conditions including Alzheimer's disease and chronic pain due to an upregulation in immune cells of the brain—microglia^{4–7}.

Recent technological advances in the field of molecular biology brought compelling evidence for neuronal *Cnr2* expression. Using RNAScope⁸, *Cnr2* was detected on excitatory and inhibitory neurons in the hippocampus^{9,10}. Furthermore, neuronal *Cnr2* expression has been found in the ventral tegmental area, prefrontal cortex, cerebellum, dorsal striatum and nucleus accumbens^{11–13}.

Acute activation of brain CB₂R reduces inhibitory synaptic transmission in the rat medial entorhinal area and neuronal excitability in the hippocampus^{9,14}, whereas chronic activation increases excitatory synaptic transmission¹⁵. The constitutive deletion of CB₂R results in decreased excitatory synaptic transmission and a reduced magnitude of long-term potentiation^{9,16–19}. Furthermore, stimulation of CB₂R in CA2/3 hippocampal neurons, but not CA1 or dentate gyrus neurons, elicits a long-lasting hyperpolarization⁹. This hyperpolarization in the hippocampus is strictly CB₂R dependent—it can be blocked with CB₂R antagonists, can be elicited with CB₂R agonist and is absent in CB₂R knockout animals. Additionally, the hyperpolarization appears to be a cell-intrinsic self-regulatory mechanism that acts complementary to presynaptic CB₁Rs. On a network level systemic treatment with CB₂R agonist results in a decreased modulation of slow-gamma oscillation dependent on the theta oscillation amplitude in area CA3⁹. These results imply that the CB₂R-dependent hyperpolarization regulates hippocampal network activity.

However, it is unknown if this very specific form of CB₂R-dependent plasticity affects synaptic architecture in CA2/3 area of the hippocampus. In this study, we addressed this question using CB₂R-deficient mice. We show that CB₂R deletion caused a sex-specific increase in synaptic proteins in the hippocampus and altered social

Institute for Molecular Psychiatry, Medical Faculty, University Hospital Bonn, University of Bonn, Venusberg-Campus 1, Bldg. 76, 53127 Bonn, Germany. ✉email: a.zimmer@uni-bonn.de

memory. Thereby, our results provide evidence for an important role of CB₂R in social memory function and synaptic architecture.

Results

Increased synapsin-I levels and puncta size in the hippocampus after CB₂R deletion in females, but not in males. To assess general changes in synapse density and size in the hippocampus we investigated synapsin-I immunostaining in the CA1, CA2 and CA3 area. The areas were discriminated based on a staining with an antibody against RGS14, a marker for CA2 principal cells (Fig. 1A). First, we analyzed the mean grey value in all hippocampal areas (Fig. 1B). We identified a significant sex and sex × genotype interaction effect and therefore analyzed females and males individually (Supplementary Table S2). As expected, we detected a significant effect of hippocampal layer in all areas with the highest density of synapsin-I in stratum lucidum. Furthermore, we found a significant genotype effect in females in all areas of the hippocampus (Fig. 1C). Post-hoc analysis revealed significantly increased synapsin-I levels in all areas and all layers. In male mice, a genotype effect was present in the CA3 area, but posthoc analysis did not reveal any layer-specific genotype difference.

To address if the increased synapsin-I signal in females was due to an increase in the size of synaptic clusters, we analyzed the average size of synapsin-I puncta specifically in the CA2 and CA3 area (Fig. 2A). Our analysis showed an overall genotype effect in both CA2 and CA3, exclusively in females (Fig. 2B). The following posthoc analysis did not reveal any specific changes in any of the CA2 layers. However, we observed a significant increase in stratum lucidum of the CA3 hippocampal area. In contrast, no genotype effect was present in male mice.

Furthermore, we detected a layer effect in both males and females in the CA2 and CA3 area of the hippocampus with the biggest puncta size in stratum lucidum (Fig. 2B).

CB₂R deletion alters excitatory and inhibitory synapses in a sex-specific manner. We then investigated excitatory synapses in the CA areas of the hippocampus using vesicular glutamate transporter 1 (vGLUT1) as a marker. Co-staining with vGLUT1 and synapsin-I revealed a high degree of colocalization between those markers (Fig. 3A). As for synapsin-I, we found an overall layer effect and a main genotype effect in the CA2 and CA3 areas in female mice (Fig. 3B,C). However, we detected no genotype effect in the CA1 region.

The subsequent posthoc analysis in CA2 and CA3 did not reveal any layer-specific effect. In males, there was no genotype effect. Our data indicate that vGLUT1 expression was altered in female CB₂R^{-/-} mice, but the effects were not as pronounced as the changes observed for synapsin-I.

We next investigated inhibitory synapses in the hippocampus using vGAT as a marker. The extent of colocalization between synapsin-I and vGAT staining is lower when compared with what we observed for synapsin-I and vGLUT1 (Fig. 4A). Consistent with the other synaptic markers we analyzed, we found a significant layer effect across all groups. Furthermore, we detected a main effect of the genotype in both female and male mice (Fig. 4B,C). Although an increase in vGAT mean gray values was observed in both sexes of CB₂ knockout mice, it was again much more pronounced in females. A significant genotype effect was present for all areas and regions after posthoc analysis in female mice. However, male mice exhibited statistical significance only in CA1 stratum pyramidale.

CB₂R deletion decreases social memory in both male and female mice. Our synaptic marker analysis showed the most prominent changes in the CA2/3 areas. The CA2 hippocampal area is important for social memory²⁰. Hence, we investigated short-term social memory in CB₂R^{-/-} mice using the partner recognition test (PR).

CB₂R^{-/-} mice and controls displayed similar social behavior as indicated by a sociability above the 50% chance level (Fig. 5A). However, only WT mice preferred to interact with a novel partner, indicating that they remembered the familiar mouse from the previous trial (Fig. 5B). In contrast, for CB₂R^{-/-} mice the preference for the novel partner did not differ from chance level, indicating a social memory impairment in these mice (Fig. 5B).

To investigate if this genotype effect was due to a sensory defect, we performed an olfaction test. Mice from both genotypes showed a significant increase in the exploration of a urine-stained cotton swab over a water-stained swab (Supplementary Fig. S2). Overall, these data suggest that CB₂R^{-/-} impairs social memory in the PR test in both male and female mice.

Discussion

The results from this study show that deletion of CB₂R alters the synaptic architecture in the hippocampus and results in social memory deficit. Thus, despite the low level of expression of CB₂R in neurons, their signaling plays an important role in synaptic functions. Moreover, our results reveal a pronounced sex effect, with female mice showing highly significant alterations in expression of hippocampal synaptic markers, in contrast to male mice. Our findings thus add to the growing evidence of important sex-specific differences in endocannabinoid signaling²¹.

Although reports indicating an important role of CB₂R in the modulation of neuronal functions were initially met with skepticism in the research community, the accumulated evidence in arguing for such a role is now compelling. For instance, acute activation of CB₂R decreased neuronal firing frequency and reduced the excitability of neurons, whereas chronic activation leads to increased neuronal excitability^{9,19}. At the same time, CB₂R has been implicated in higher cognitive functions, as CB₂R deletion led to alterations in memory performance^{7,22–24}, with a global CB₂R deletion impairing aversive memory, but enhancing working memory^{22,24,25}.

On a cellular level, CB₂R deletion leads to a decreased excitatory transmission and decreased dendritic spine numbers in the hippocampus^{18,26}. To further investigate synaptic changes in the hippocampus after CB₂R deletion, we stained for a general presynaptic marker—synapsin-I and observed an increase in synapsin-I levels

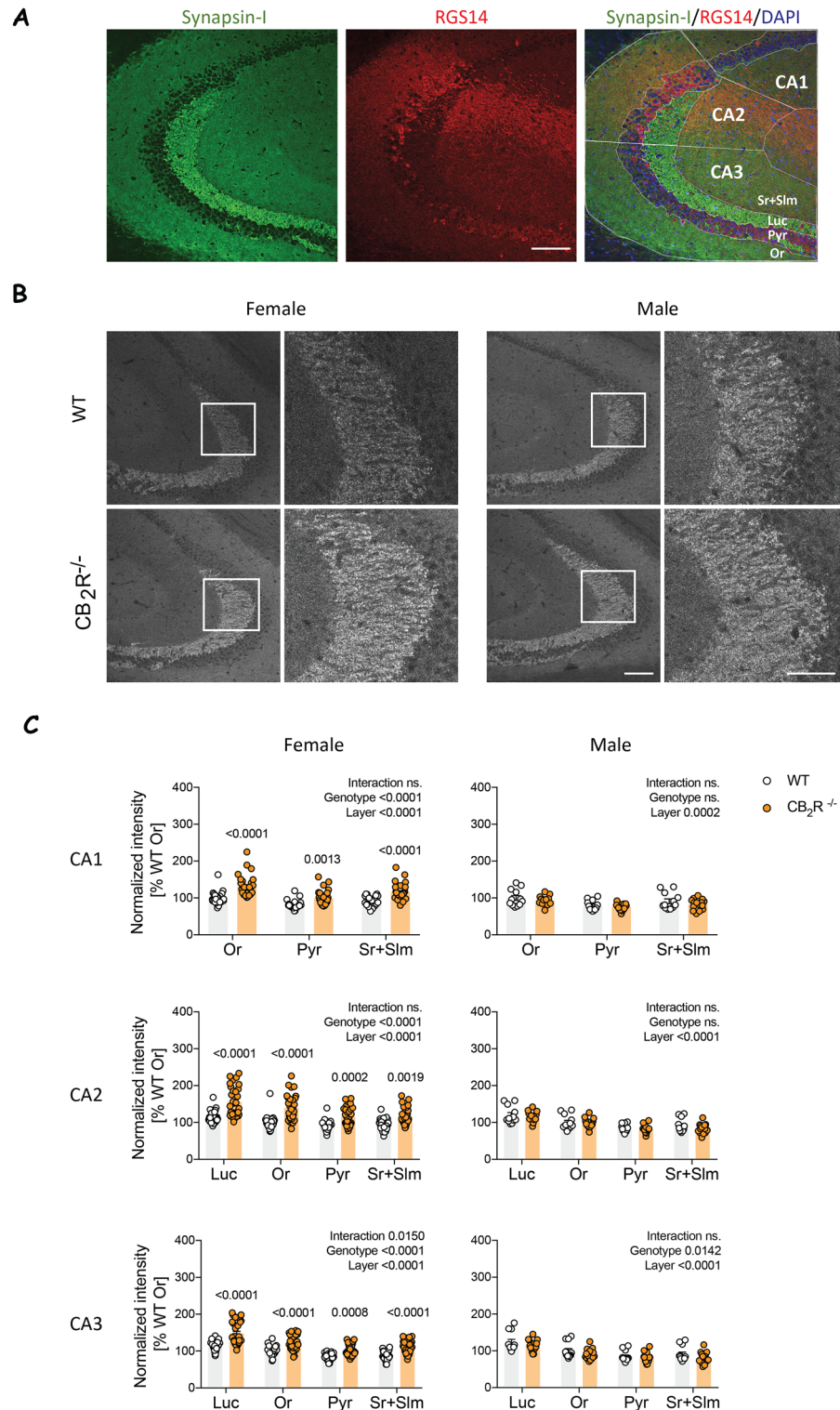


Figure 1. Synapsin-I levels are increased in the hippocampus after CB_2R deletion in female mice. (A) Example images show synapsin-I (green), RGS14 (red) and DAPI (blue). White lines indicate manual delineation of CA regions and layers in the hippocampus. Scale bar: 100 μ m. (B) Example images of synapsin-I immunoreactivity in male and female from WT and $CB_2R^{-/-}$ mice. The white box within the left panel indicates the section that is displayed in higher magnification on the right. Scale bar: 100 μ m, 50 μ m (inset). (C) Quantification of synapsin-I mean grey value within each hippocampal layer normalized to the result from stratum oriens (Or). Or stratum oriens, Luc stratum lucidum, Pyr stratum pyramidale, Sr + Slm stratum radiatum and stratum lacunosum-moleculare. White circle—WT; orange circle— $CB_2R^{-/-}$ mice. Each datapoint represents one image. Left panel—female mice (WT: n = 30 images from N = 9 mice; $CB_2R^{-/-}$: n = 31 images from N = 9 mice); right panel—male mice (WT: n = 12 images from N = 3 mice; $CB_2R^{-/-}$: n = 16 images from N = 4 mice). Top panel—CA1 region; middle panel—CA2 region; bottom panel—CA3 region. Data is displayed as mean value \pm SEM. Data was analyzed by two-way ANOVA followed by Sidak's multiple comparison test. The exact p-values are indicated on the graph and reported in Supplementary Table S1.

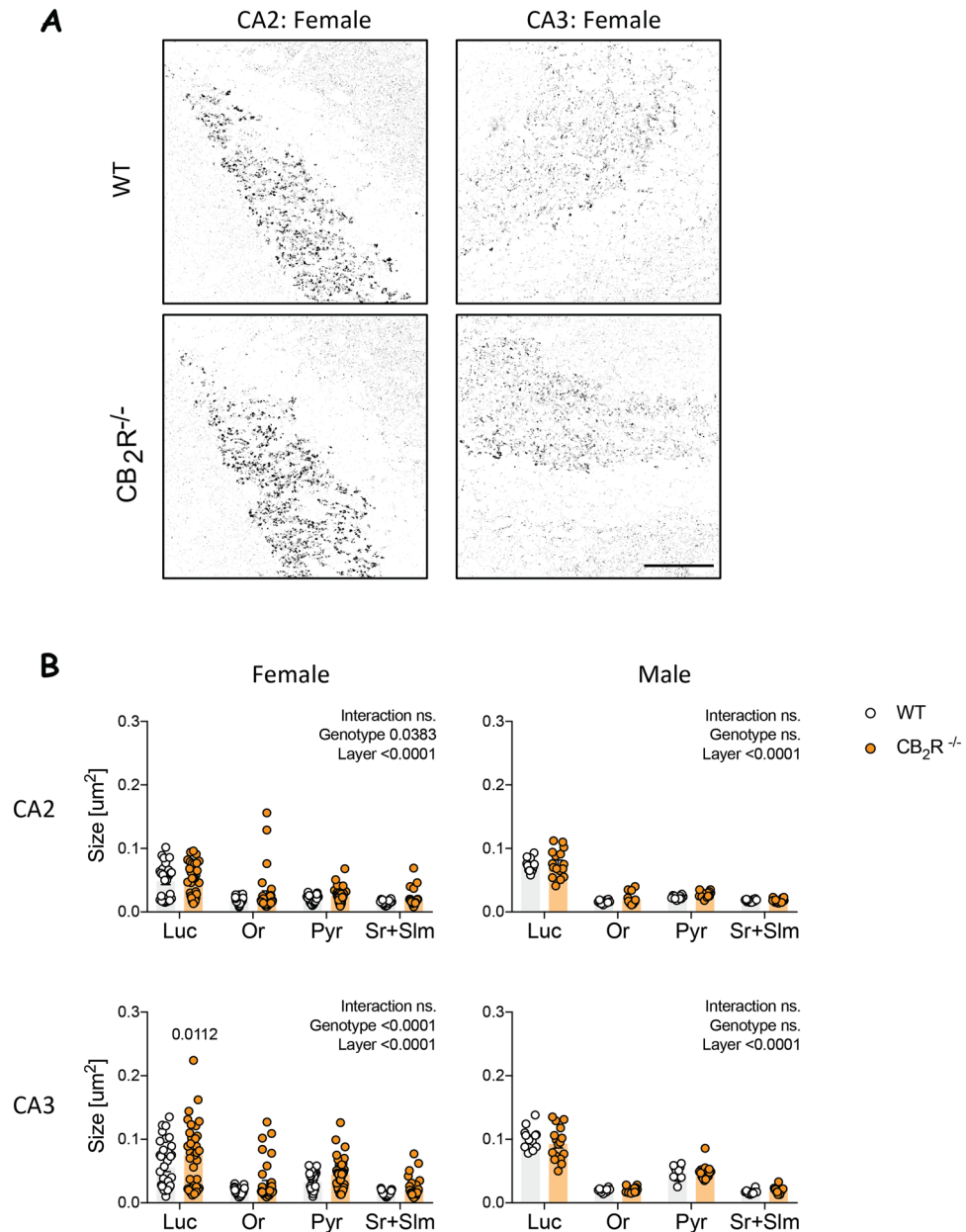


Figure 2. Average size of synapsin-I particles is increased after CB₂R deletion in females. **(A)** Example images show binary image of synapsin-I. Scale bar: 50 μm . **(B)** Quantification of synapsin-I mean puncta size (detected puncta >0.005 μm). *Or* stratum oriens, *Luc* stratum lucidum, *Pyr* stratum pyramidale, *Sr+SIm* stratum radiatum and stratum lacunosum-moleculare. White circle—WT; orange circle—CB₂R^{-/-} mice. Each datapoint represents one image. Left panel—female mice (WT: n = 28–35 images from N = 9 mice; CB₂R^{-/-}: n = 31–36 images from N = 9 mice); right panel—male mice (WT: n = 12 images from N = 3 mice; CB₂R^{-/-}: n = 16 images from N = 4 mice). Top panel—CA2 region; bottom panel—CA3 region. Data is displayed as mean value \pm SEM. Data was analyzed by two-way ANOVA followed by Sidak's multiple comparison test. The exact p-values are indicated on the graph and reported in Supplementary Table S1.

exclusively in CB₂R^{-/-} female mice. The change in synapsin-I intensity was accompanied by an increase in synapsin-I average puncta size in both CA2 and CA3 area of the hippocampus. It is possible that an increase in the presynaptic vesicle pool is a compensatory mechanism to counteract the decreased number of dendritic spines. On the other hand, synapsins have been shown to boost synaptic release at high firing rates by recruiting more vesicles from the reserve vesicle pool at excitatory synapses²⁷. Whether the observed increase comes from an increase in overall vesicle number or an alteration in synaptic facilitation should be addressed in the future. In addition, loss of synapsin-I decreases baseline transmission at inhibitory synapses²⁷. In agreement with that, decreasing synapsin-I expression also decreases the pool of readily releasable synaptic vesicles and alters

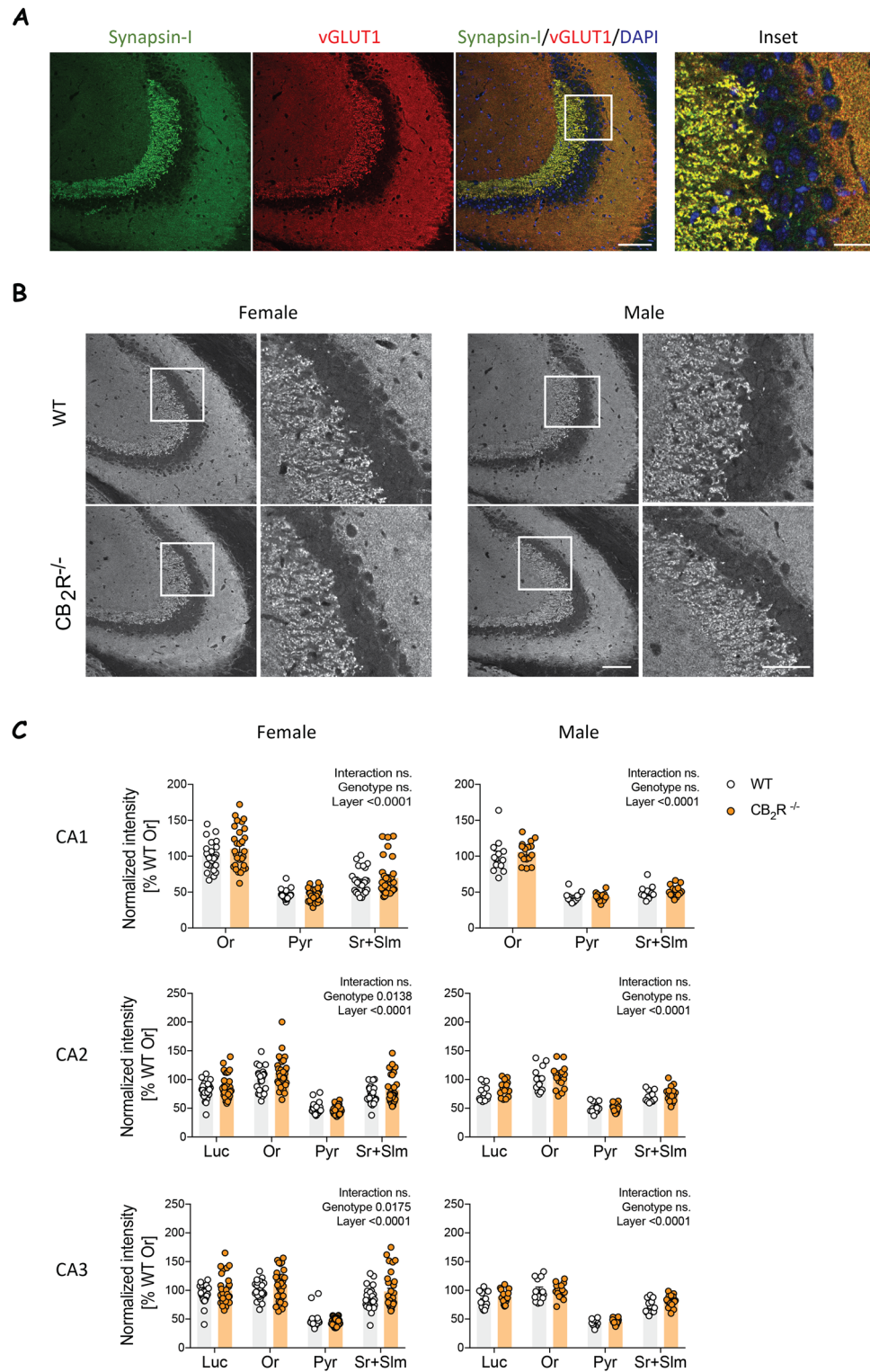


Figure 3. vGLUT1 levels are slightly increased in female CB₂R^{-/-} mice. **(A)** Example images show synapsin-I (green), vGLUT1 (red) and DAPI (blue). Scale bar: 100 μm, 25 μm (inset). **(B)** Example images of vGLUT1 immunoreactivity in male and female from WT and CB₂R^{-/-} mice. The white box within the left panel indicates the section that is displayed in higher magnification on the right. Scale bar: 100 μm, 50 μm (inset). **(C)** Quantification of vGLUT1 mean grey value within each hippocampal layer normalized to the result from stratum oriens (Or). Or stratum oriens, Luc stratum lucidum, Pyr stratum pyramidale, Sr + SIm stratum radiatum and stratum lacunosum-moleculare. White circle—WT; orange circle—CB₂R^{-/-} mice. Each datapoint represents one image. Left panel—female mice (WT: n = 30 images from N = 9 mice; CB₂R^{-/-}: n = 31 images from N = 9 mice); right panel—male mice (WT: n = 12 images from N = 3 mice; CB₂R^{-/-}: n = 16 images from N = 4 mice). Top panel—CA1 region; middle panel—CA2 region; bottom panel—CA3 region. Data is displayed as mean value ± SEM. Data was analyzed by two-way ANOVA followed by Sidak's multiple comparison test. The exact p-values are indicated on the graph and reported in Supplementary Table S1.

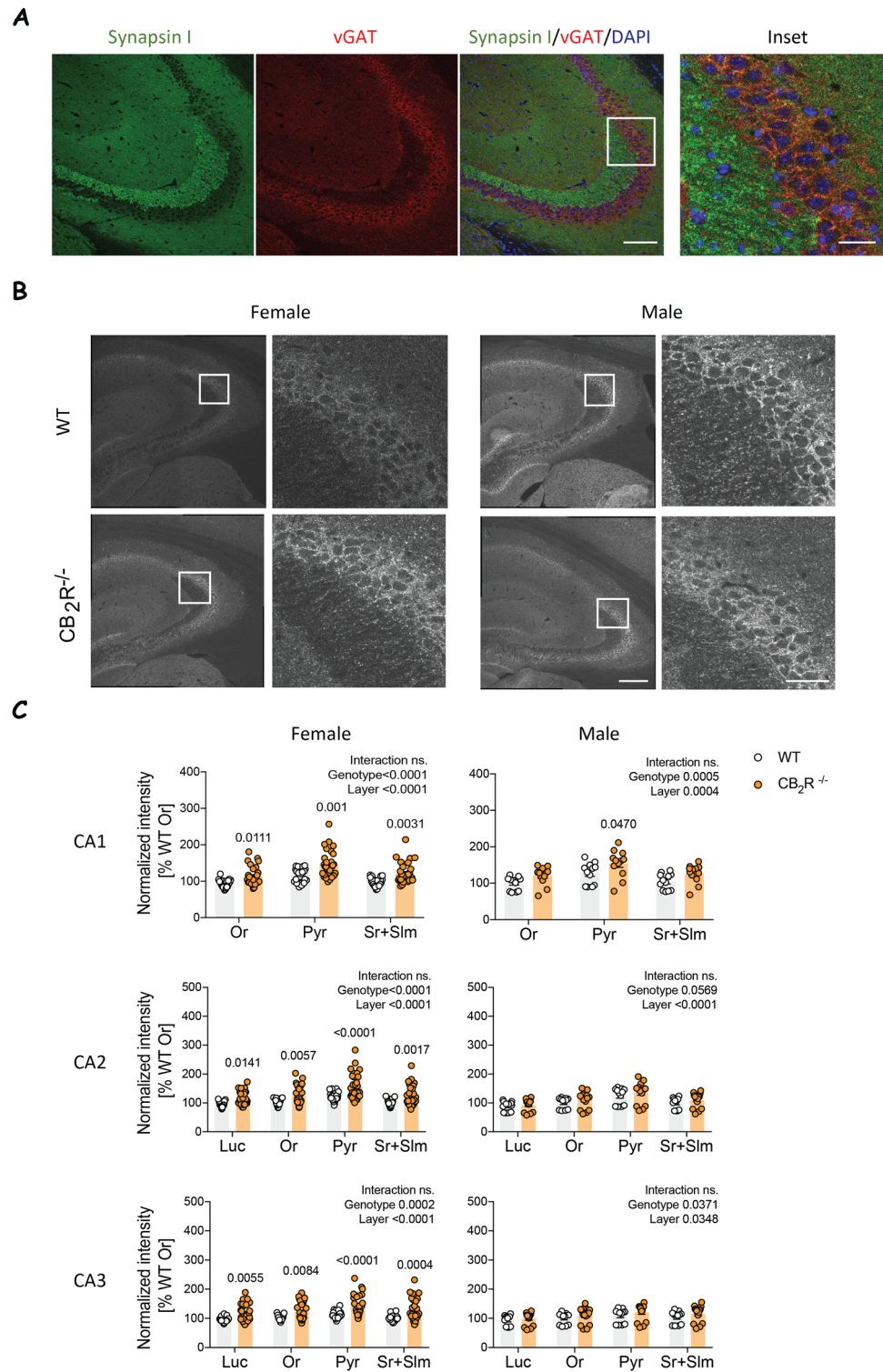


Figure 4. vGAT levels are increased in female CB₂R^{-/-} mice. **(A)** Example images show synapsin-I (green), vGAT (red) and DAPI (blue). Scale bar: 100 μm, 25 μm (inset). **(B)** Example images of vGAT immunoreactivity in male and female from WT and CB₂R^{-/-} mice. The white box within the left panel indicates the section that is displayed in higher magnification on the right. Scale bar: 200 μm, 25 μm (inset). **(C)** Quantification of vGAT mean grey value within each hippocampal layer normalized to the result from stratum oriens (Or). Or stratum oriens, Luc stratum lucidum, Pyr stratum pyramidale, Sr + Slm stratum radiatum and stratum lacunosum-moleculare. White circle—WT; orange circle—CB₂R^{-/-} mice. Each datapoint represents one image. Left panel—female mice (WT: n = 30 images from N = 9 mice; CB₂R^{-/-}: n = 31 images from N = 9 mice); right panel—male mice (WT: n = 12 images from N = 3 mice; CB₂R^{-/-}: n = 16 images from N = 4 mice). Top panel—CA1 region; middle panel—CA2 region; bottom panel—CA3 region. Data is displayed as mean value ± SEM. Data was analyzed by two-way ANOVA followed by Sidak’s multiple comparison test. The exact p-values are indicated on the graph and reported in Supplementary Table S1.

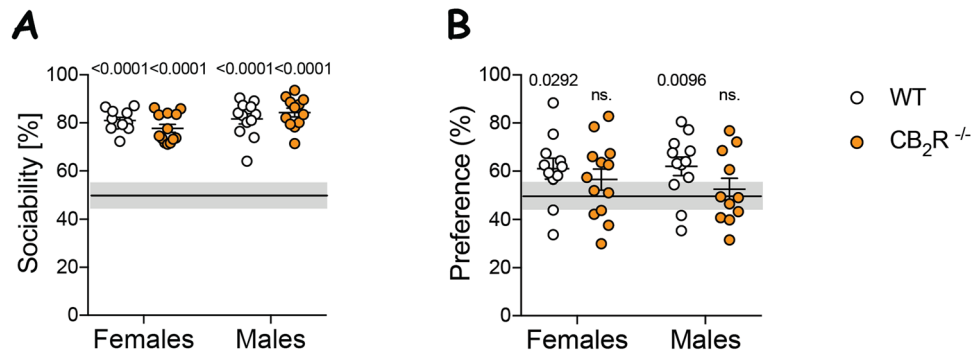


Figure 5. CB₂R deletion decreases social memory in both male and female mice. **(A)** Sociability (%) was calculated as interaction time with a partner mouse over total interaction time. A mean value above 50% indicates that the mice are social. **(B)** Preference (%) for the novel partner was calculated as time with the novel partner mouse over total interaction time. Significant difference from the chance level (50%) indicates learning. White circle—WT; orange circle—CB₂R^{-/-} mice. Squares represent data from individual mice (N = 11–13 mice/sex/genotype). Data are displayed as mean value ± SEM. Each group was analyzed individually by one-sample t-test (hypothetical mean = 50). The exact p-values are indicated on the graph.

short-term synaptic plasticity, while not affecting memory or long-term potentiation in young mice^{28–31}. Thus, an increase in synapsin-I could explain the improved working memory in CB₂R^{-/-} mice²⁴.

Alterations in synapsins are known to affect both excitatory and inhibitory synapses although in a different capacity. Furthermore, *Cnr2* has been detected on both excitatory and inhibitory cells¹⁰. Following the discovery of increased synapsin-I levels in females, we asked if the increase in presynaptic vesicle staining was due to alterations in glutamatergic or GABAergic synapses. Both vGLUT1 and vGAT intensities were enhanced in CB₂R^{-/-} female mice, suggesting that both excitatory and inhibitory synapses are regulated by CB₂R.

We observed a stronger effect for inhibitory synapses. It is known that even subtle alterations in perisomatic inhibitory synapses go along with perturbations in gamma oscillations³². Thus, our findings might explain the observed CB₂R-dependent alterations of gamma oscillations⁹. However, we do see changes in both excitatory and inhibitory synapses and those changes seem to be prominent in all hippocampal layers and most hippocampal regions. Therefore, it is likely that these marker proteins are not directly regulated by CB₂R activity but rather reflect an overall change in the synaptic landscape of the hippocampus. Furthermore, our data indicate that CB₂R modulates hippocampal networks differently in males and females.

In light of these sex-specific phenotypes, it is important to note that most of the previous studies performed on CB₂R knockouts were done with sex-mixed groups^{7,24,33–35} or exclusively with male mice^{18,22,25,36–38}. It is therefore possible that sex-specific phenotypes have been overlooked and that the relevance for CB₂R-dependent processes in the central nervous system have been underestimated. It is not clear why females have a stronger CB₂R knockout phenotype, but these sex differences may be related to differential CB₂R expression levels. It has been already shown that *Cnr2* expression in the hippocampus, prefrontal cortex and hypothalamus is higher in female than in male mice³⁹.

We also evaluated social behavior and social memory in this study because Stempel et al. described a CB₂R-dependent hyperpolarization phenomenon in CA2/3 area⁹. The CA2 area in particular has been implicated in social memory²⁰. Indeed, we observed that short-term social memory was impaired in both female and male CB₂R^{-/-} mice. Further studies deleting CB₂R specifically in the CA2 region, are necessary to elucidate CB₂R functions in hippocampal neurocircuits in more detail. Such studies are important because the pronounced cognitive phenotype after CB₂R deletion now clearly reveals a significant role of CB₂R in the modulation of different forms of memory, despite its low expression levels.

Materials and methods

Animals. The experiments were carried out with 4–6-month old female and male mice. Food and water were provided ad libitum. To investigate the results of the constitutive *Cnr2* deletion, we compared B6.Cg-*Cnr2*^{tm1Zim} (CB₂R^{-/-}; MGI Cat# 2663848, RRID: MGI:2663848)⁴⁰ with C57BL/6/J (WT) mice. CB₂R^{-/-} were generated using homologous recombination and have a constitutive 131 amino acid deletion at the C-terminus of the CB₂R eliminating part of the intracellular loop 3 and transmembrane domains 6 and 7⁴⁰. Among others, CB₂R^{-/-} have impaired neuromodulatory functions, accelerated age-dependent bone loss and obesity^{40–42}. Recently, CB₂R^{-/-} mice were also reported to have aversive memory impairment^{22,24,25}.

Care of the animals and conduction of the experiments followed the guidelines of the European Communities Directive 86/609/EEC and the German Animal Protection Law regulating animal research and were approved by the ethics committee of the Landesamt für Natur, Umwelt und Verbraucherschutz Nordrhein-Westfalen (LANUV NRW), Germany (AZ 84-02.04.2017.A231). The experiments were carried out in accordance with ARRIVE guidelines. Independent groups were used for behavioral testing and immunohistochemical analysis. For behavioral testing, an independent male and female groups were used (N = 11–13 mice/group). For immunohistological analysis two independent groups of mice were used. One group included male (N = 3–4 mice/

genotype) and female (N = 4 mice/genotype) mice from WT and CB₂R^{-/-}. Another group included only female mice (N = 4–5 mice/genotype).

Behavioral testing. A male and a female group were tested independently with 11–13 mice/sex/genotype. The experimenter was blind with regards to the genotype. A week before the first test, mice were single-housed and transferred to a room with a reversed light–dark cycle (lights off at 9:00 a.m.). Behavioral tests were conducted during the dark phase (from around 9:30 a. m.).

Partner recognition test (PR). This paradigm was used to assess social memory. Animal activity was recorded with the EthoVision XT 13 (Noldus, RRID:SCR_000441). The test was performed in an open-field box (44 cm × 44 cm) containing a 1 cm layer of sawdust under dim illumination. For three consecutive days, mice were allowed to explore the arena freely for 10 min and were habituated to the environment. On the test day, mice underwent two trials. In trial 1, mice were given 9 min to freely explore the arena containing an object (metal can) and a grid cage (diameter around 10 cm, height around 12 cm) with an unfamiliar C57BL/6J male partner mouse. The can and the cage were in opposite corners, each placed around 6–7 cm from the wall. Partner mice were approximately 10 weeks old. Interaction was noted when the mouse nose point was within 2 cm of the cage/can. The time spent on top of any of the objects was deduced from the interaction time. After trial 1, mice were put back to their homecages for 1 h. Sociability in trial 1 was calculated as follows: sociability (%) = $T_p / (T_p + T_c) \times 100$, where T_p is the time of interaction with a partner mouse and T_c is the time of interaction with the object. To detect if the sociability of the group was greater than the chance level, the mean sociability value was tested with a one-sample t-test against a hypothetical mean (50%) representing the chance level. Sociability above 50% indicated that the mouse spent more time interacting with a partner than with an object. In trial 2, the metal can was replaced by a grid cage with a novel partner mouse and the test mouse was given 3 min to freely explore and interact with both partners. Preference for the novel partner was calculated as preference (%) = $T_n / (T_f + T_n) \times 100$, where T_f is the time spent with the familiar partner and T_n is the time spent with a novel partner mouse. If the mouse recognized its previous partner, it should have spent > 50% of interaction time interacting with a novel partner. Therefore, a preference for the new partner is interpreted as learning. To detect learning in each group, the preference for the novel partner was tested with a one-sample t-test against a hypothetical mean (50%) to detect if it statistically deviates from the chance level.

Brain isolation. Two independent cohorts of mice were transcardially perfused with phosphate-buffered saline (PBS). Brains were isolated and hemisected. One of the hemispheres was postfixed in 4% formaldehyde (pH = 6.9; Sigma- Aldrich) for 3.5–4 h on ice, shaking. They were cryoprotected using overnight incubation in 10% sucrose followed by an overnight incubation in 30% sucrose. Brains were frozen in dry ice-cooled isopentane and stored at – 80 °C until sectioning.

Immunohistochemistry. Frozen-fixed hemispheres were cut with a cryostat (Microm HM500) into 20 µm sections and stored at – 20 °C. Prior to the staining, slices were thawed on a 37 °C heating plate for 30 min. They were then permeabilized for 10 min in 0.3% Triton X-100 in Tris- buffered saline (1 M TBS, pH = 7.5), followed by 3 × 5 min wash in TBS. Then, antigen retrieval in citrate buffer pH = 6 for 20 min at 65 °C was performed. The slides were washed 3 times with TBS and blocked for 1 h in blocking buffer (2% BSA, 10% normal goat serum, 0.3% Triton X-100 in TBS). Afterwards, the slides were incubated overnight with primary antibodies in blocking buffer: 1:250 rabbit anti-synapsin-I (Abcam Cat# ab64581, RRID:AB_1281135), 1:1000 guinea pig anti-vGLUT1 (Millipore Cat# AB5905, RRID:AB_2301751), 1:200 guinea pig anti-vGAT (Synaptic Systems Cat# 131 004, RRID:AB_887873), 1:5 mouse anti-RGS14 (Antibodies Incorporated Cat# 73-170, RRID:AB_10698026). The next day, the slides were incubated for 20 min at room temperature and washed 3 times in TBS. Then they were blocked for 1 h followed by an incubation with 1:1000 AlexaFluor[®] conjugated secondary antibodies in blocking solution: goat anti-mouse AF568 (Molecular Probes Cat# A-11031, RRID:AB_144696), goat anti-rabbit AF488 (Molecular Probes Cat# A-11008, RRID:AB_143165), goat anti-guinea pig AF647 (Abcam Cat# ab150187, RRID:AB_2827756). Afterwards, the slides were washed 3 times in TBS, stained for 4',6-Diamidin-2-phenylindol (DAPI), washed once in TBS and mounted using ProLong[™] Diamond Antifade Mountant (Life technologies, P36961).

Image acquisition and analysis. The experimenter was blind with regards to the genotype during image acquisition and analysis. Single-plane confocal pictures were obtained with a LeicaSP8 inverted confocal microscope equipped with a 20× water immersion objective (N.A. 0.75). For synaptic quantification high-magnification single-plane confocal images of hippocampal areas were obtained using a LeicaSP8 inverted confocal microscope and a 63× water immersion objective (N.A. 1.2). The imaging conditions were defined once for each staining and kept during all imaging sessions. For presentation, images were post-processed in ImageJ to adjust brightness and contrast. For quantification, images were analyzed using ImageJ. All regions of interest (ROI) were delineated manually using RGS14/DAPI/synapsin-I merged image. In 20× and 63× images, the mean grey value was measured within each ROI. For particle analysis images were thresholded using a fixed mean grey value threshold to obtain a binary image. An appropriate threshold per staining was determined as a mean of manual thresholds set for all the pictures. The same threshold was applied to all images and genotypes within a staining. The number and average size of puncta per ROI was counted using Image J's 'Analyze Particles' function (minimum puncta size: 0.005 µm). For each animal 3–4 images were taken. Data were normalized as % of mean of control group (stratum oriens). Data from immunohistological groups were pooled together per sex. Mean

per animal was included in Supplementary Fig. S1 and the corresponding statistical analysis in Supplementary Table 3.

Statistical analysis and data presentation. Microsoft Excel was used for data analysis followed by statistical analysis and data visualization in GraphPad Prism version 7.0.0 and 9.1.2 for Mac, GraphPad Software, San Diego, California USA, www.graphpad.com. Figures were put together in Adobe Illustrator 2020. Behavioral data analysis was done using EthoVision XT 13 (Noldus, RRID:SCR_000441). For immunohistological data two-way ANOVA was used (independent variables: genotype and layer) followed by Sidak's multiple comparison test. To identify differences between sexes in Synapsin-I levels, three-way ANOVA was used (independent variables: genotype, sex and layer; Supplementary Table S2). For PR, one-sample t-test was used to test the mean of the group against a theoretical mean of 50 to detect significant difference of each group from the chance level. Statistical significance was stated when p -value < 0.05 at a 95% confidence interval.

Data availability

Datasets are available on request. The raw data supporting the conclusions of this article will be made available by the authors, without undue reservation, to any qualified researcher.

Received: 22 April 2021; Accepted: 26 July 2021

Published online: 19 August 2021

References

- Galiègue, S. *et al.* Expression of central and peripheral cannabinoid receptors in human immune tissues and leukocyte subpopulations. *Eur. J. Biochem.* **232**, 54–61 (1995).
- Schatz, A. R., Lee, M., Condie, R. B., Pulaski, J. T. & Kaminski, N. E. Cannabinoid receptors CB1 and CB2: A characterization of expression and adenylate cyclase modulation within the immune system. *Toxicol. Appl. Pharmacol.* **142**, 278–287 (1997).
- Zhang, H. Y. *et al.* CB2 receptor antibody signal specificity: Correlations with the use of partial CB2-knockout mice and anti-rat CB2 receptor antibodies. *Acta Pharmacol. Sin.* **40**, 398–409 (2019).
- López, A. *et al.* Cannabinoid CB2 receptors in the mouse brain: Relevance for Alzheimer's disease. *J. Neuroinflamm.* **15**, 1–11 (2018).
- Benito, C. *et al.* Cannabinoid CB2 receptors and fatty acid amide hydrolase are selectively overexpressed in neuritic plaque-associated glia in Alzheimer's disease brains. *J. Neurosci.* **23**, 11136–11141 (2003).
- Beltramo, M. *et al.* CB2 receptor-mediated antihyperalgesia: Possible direct involvement of neural mechanisms. *Eur. J. Neurosci.* **23**, 1530–1538 (2006).
- Schmöle, A. C. *et al.* Cannabinoid receptor 2 deficiency results in reduced neuroinflammation in an Alzheimer's disease mouse model. *Neurobiol. Aging* **36**, 710–719 (2015).
- Wang, F. *et al.* RNAscope: A novel in situ RNA analysis platform for formalin-fixed, paraffin-embedded tissues. *J. Mol. Diagn.* **14**, 22–29 (2012).
- Stempel, A. V. *et al.* Cannabinoid type 2 receptors mediate a cell type-specific plasticity in the hippocampus. *Neuron* **90**, 795–809 (2016).
- Li, Y. & Kim, J. Neuronal expression of CB2 cannabinoid receptor mRNAs in the mouse hippocampus. *Neuroscience* **311**, 253–267 (2015).
- Jordan, C. J. & Xi, Z.-X. Progress in brain cannabinoid CB2 receptor research: From genes to behavior. *Neurosci. Biobehav. Rev.* **176**, 139–148 (2019).
- Zhang, H. Y. *et al.* Species differences in cannabinoid receptor 2 and receptor responses to cocaine self-administration in mice and rats. *Neuropsychopharmacology* **40**, 1037–1051 (2015).
- Liu, Q. R. *et al.* Cannabinoid type 2 receptors in dopamine neurons inhibits psychomotor behaviors, alters anxiety, depression and alcohol preference. *Sci. Rep.* **7**, 1–17 (2017).
- Morgan, N. H., Stanford, I. M. & Woodhall, G. L. Functional CB2 type cannabinoid receptors at CNS synapses. *Neuropharmacology* **57**, 356–368 (2009).
- Kim, J. & Li, Y. Chronic activation of CB2 cannabinoid receptors in the hippocampus increases excitatory synaptic transmission. *J. Physiol.* **4**, 871–886 (2015).
- Zhang, H.-Y. *et al.* Cannabinoid CB2 receptors modulate midbrain dopamine neuronal activity and dopamine-related behavior in mice. *Proc. Natl. Acad. Sci.* **111**, E5007–E5015 (2014).
- Andó, R. D., Bíró, J., Csölle, C., Ledent, C. & Sperlágh, B. The inhibitory action of exo- and endocannabinoids on [3H]GABA release are mediated by both CB1 and CB2 receptors in the mouse hippocampus. *Neurochem. Int.* **60**, 145–152 (2012).
- Li, Y. & Kim, J. Deletion of CB2 cannabinoid receptors reduces synaptic transmission and long-term potentiation in the mouse hippocampus. *Hippocampus* **26**, 275–281 (2016).
- den Boon, F. S. *et al.* Excitability of prefrontal cortical pyramidal neurons is modulated by activation of intracellular type-2 cannabinoid receptors. *Proc. Natl. Acad. Sci.* **109**, 3534–3539 (2012).
- Hitti, F. L. & Siegelbaum, S. A. The hippocampal CA2 region is essential for social memory. *Nature* **508**, 88–92 (2014).
- Wagner, E. J. Sex differences in cannabinoid-regulated biology: A focus on energy homeostasis. *Front. Neuroendocrinol.* **40**, 101–109 (2016).
- García-Gutiérrez, M. S. *et al.* Synaptic plasticity alterations associated with memory impairment induced by deletion of CB2 cannabinoid receptors. *Neuropharmacology* **73**, 388–396 (2013).
- Li, X. M., Suchland, K. L. & Ingram, X. S. L. Compensatory activation of cannabinoid CB2 receptor inhibition of GABA release in the rostral ventromedial medulla in inflammatory pain. *J. Neurosci.* **37**, 626–636 (2017).
- Li, Y. & Kim, J. CB2 cannabinoid receptor knockout in mice impairs contextual long-term memory and enhances spatial working memory. *Neural Plast.* **2016**, 1–14 (2016).
- Ortega-Alvaro, A., Aracil-Fernández, A., García-Gutiérrez, M. S., Navarrete, F. & Manzanera, J. Deletion of CB2 cannabinoid receptor induces schizophrenia-related behaviors in mice. *Neuropsychopharmacology* **36**, 1489–1504 (2011).
- García-gutiérrez, M. S. *et al.* Neuropharmacology synaptic plasticity alterations associated with memory impairment induced by deletion of CB2 cannabinoid receptors. *Neuropharmacology* **73**, 388–396 (2013).
- Gitler, D. *et al.* Different presynaptic roles of synapsins at excitatory and inhibitory synapses. *J. Neurosci.* **24**, 11368–11380 (2004).
- Baldelli, P., Fassio, A., Valtorta, F. & Benfenati, F. Lack of synapsin I reduces the readily releasable pool of synaptic vesicles at central inhibitory synapses. *J. Neurosci.* **27**, 13520–13531 (2007).
- Rosahl, T. W. *et al.* Short-term synaptic plasticity is altered in mice lacking synapsin I. *Cell* **75**, 661–670 (1993).

30. Kushner, S. A. *et al.* Modulation of presynaptic plasticity and learning by the H-ras/extracellular signal-regulated kinase/synapsin I signaling pathway. *J. Neurosci.* **25**, 9721–9734 (2005).
31. Corradi, A. *et al.* Synapsin-I- and synapsin-II-null mice display an increased age-dependent cognitive impairment. *J. Cell Sci.* **121**, 3042–3051 (2008).
32. Hammer, M. *et al.* Perturbed hippocampal synaptic inhibition and γ -oscillations in a neurologin-4 knockout mouse model of autism. *Cell Rep.* **13**, 516–523 (2015).
33. Li, Y. & Kim, J. Distinct roles of neuronal and microglial CB2 cannabinoid receptors in the mouse hippocampus. *Neuroscience* **363**, 11–25 (2017).
34. Bouchard, J. *et al.* Cannabinoid receptor 2 signaling in peripheral immune cells modulates disease onset and severity in mouse models of Huntington's disease. *J. Neurosci.* <https://doi.org/10.1523/jneurosci.4008-12.2012> (2012).
35. Koppel, J. *et al.* CB2 receptor deficiency increases amyloid pathology and alters tau processing in a transgenic mouse model of Alzheimer's disease. *Mol. Med.* **19**, 357–364 (2013).
36. Aso, E., Andrés-Benito, P., Carmona, M., Maldonado, R. & Ferrer, I. Cannabinoid receptor 2 participates in amyloid- β processing in a mouse model of Alzheimer's disease but plays a minor role in the therapeutic properties of a cannabis-based medicine. *J. Alzheimer's Dis.* **51**, 489–500 (2016).
37. Navarrete, F. *et al.* Role of CB2 cannabinoid receptors in the rewarding, reinforcing, and physical effects of nicotine. *Neuropsychopharmacology* **38**, 2515–2524 (2013).
38. La Porta, C., Bura, S. A., Aracil-Fernández, A., Manzanares, J. & Maldonado, R. Role of CB1 and CB2 cannabinoid receptors in the development of joint pain induced by monosodium iodoacetate. *Pain* **154**, 160–174 (2013).
39. Xing, G. *et al.* Differential expression of brain cannabinoid receptors between repeatedly stressed males and females may play a role in age and gender-related difference in traumatic brain injury: Implications from animal studies. *Front. Neurol.* **5**, 1–12 (2014).
40. Buckley, N. E. *et al.* Immunomodulation by cannabinoids is absent in mice deficient for the cannabinoid CB2 receptor. *Eur. J. Pharmacol.* **396**, 141–149 (2000).
41. Ofek, O. *et al.* Peripheral cannabinoid receptor, CB2, regulates bone mass. *Proc. Natl. Acad. Sci. U. S. A.* **103**, 696–701 (2006).
42. Agudo, J. *et al.* Deficiency of CB2 cannabinoid receptor in mice improves insulin sensitivity but increases food intake and obesity with age. *Diabetologia* **53**, 2629–2640 (2010).

Acknowledgements

We would like to thank Eva Drews for assistance with animal test proposals. We would like to thank Daniel Müller-Komorowska for proof reading and Anne Zimmer and Edda Erxlebe for the technical assistance with genotyping and perfusions. Joanna Agnieszka Komorowska-Müller was supported in part by the International Max Planck Research School for Brain and Behavior. Andreas Zimmer is member of the Cluster of Excellence ImmunoSensation, funded by the Deutsche Forschungsgemeinschaft (DFG, German Research Foundation) under Germany's Excellence Strategy—EXC2151—390873048.

Author contributions

B.S., J.A.K.M. and A.Z. designed the project. J.A.K.M. performed all the experiments, collected the data, analyzed and visualized the data. J.A.K.M. and K.A.R. imaged and analyzed the immunohistochemistry data. B.S. and A.Z. supervised the work. A.Z. provided funding. J.A.K.M. and A.Z. wrote the initial manuscript to which all authors contributed. All authors accepted the final manuscript.

Funding

Open Access funding enabled and organized by Projekt DEAL.

Competing interests

The authors declare no competing interests.

Additional information

Supplementary Information The online version contains supplementary material available at <https://doi.org/10.1038/s41598-021-96285-9>.

Correspondence and requests for materials should be addressed to A.Z.

Reprints and permissions information is available at www.nature.com/reprints.

Publisher's note Springer Nature remains neutral with regard to jurisdictional claims in published maps and institutional affiliations.



Open Access This article is licensed under a Creative Commons Attribution 4.0 International License, which permits use, sharing, adaptation, distribution and reproduction in any medium or format, as long as you give appropriate credit to the original author(s) and the source, provide a link to the Creative Commons licence, and indicate if changes were made. The images or other third party material in this article are included in the article's Creative Commons licence, unless indicated otherwise in a credit line to the material. If material is not included in the article's Creative Commons licence and your intended use is not permitted by statutory regulation or exceeds the permitted use, you will need to obtain permission directly from the copyright holder. To view a copy of this licence, visit <http://creativecommons.org/licenses/by/4.0/>.

© The Author(s) 2021